- Supporting Information -

Fundamental limit of the emission linewidths of quantum dots: an ab initio study of CdSe nanocrystals

Sungwoo Kang,[1] Yongwook Kim,[2] Eunjoo Jang,[2] Youngho Kang,[3*] and Seungwu Han[1*]*

[1]Department of Materials Science and Engineering, Seoul National University, Seoul 08826, Korea.

[2]Inorganic Material Lab, Samsung Advanced Institute of Technology, Samsung Electronics, Gyeonggi-do 16678, Korea.

[3]Department of Materials Science and Engineering, Incheon National University, Incheon 22012, Korea.

Corresponding Author

*E.J.: E-mail: ejjang12@samsung.com

*Y.K.: E-mail: youngho84@inu.ac.kr

*S.H.: E-mail: hansw@snu.ac.kr

Calculation details

The density functional theory (DFT) calculations are performed by Vienna *ab initio* simulation package (VASP) [S1] with projector augmented waves (PAW) [S2]. The cutoff energy is set to 300 eV that ensures the convergence of the total energy within 2 meV/atom. Further increase of the cutoff energy up to 400 eV rarely changes the spectral linewidth and reorganization energy (E_{re}) of CdSe NC, as shown in Table S2. The atomic geometries are optimized until all the atomic forces are less than 0.001 eV/Å. The lattice parameter of the simulation cell is set so that the minimum distance between atoms between periodic images is about 15 Å. We employ the generalized gradient approximation (GGA) functional with Hubbard U corrections [S3,S4]. The effective on-site interaction energy of Cd 4d electrons are set to U–J = 9.5 eV. This value of U–J is chosen to provide similar value of S_{eff} to hybrid functional (Figure S5) which gives similar band gap of CdSe NCs to the experiment (Figure S4). The vibrational eigenmodes are calculated using a finite-difference method with displacement of 0.015 Å. Note that GGA+U functional well reproduces the experimental lattice parameters of bulk wurtize and zinc-blende CdSe (Table S3), phonon band diagram of bulk WZ CdSe (Figure S10a), and phonon density of states of tetrahedral zinc-blende CdSe NCs (Figure S10b). The mass of pseudo-hydrogen atoms is set to 16 amu following previous study [S5], but the choice of hydrogen-mass does not affect calculation results of FWHM (Table S4). Several imaginary modes are found in the calculation of vibrational eigenmodes for some structures. However, these modes are associated with vibrations of pseudo-hydrogen ligands which do not contribute to the exciton-phonon coupling of NCs, and therefore, we neglect them. HR factors in tests calculations (Figures S2, S3, S5, S6) are evaluated based on force differences, i.e., the harmonic approximation, instead of atomic displacements (ref. S6). Chemical formula and calculation parameters used to obtain line spectra are stated in Table S5.

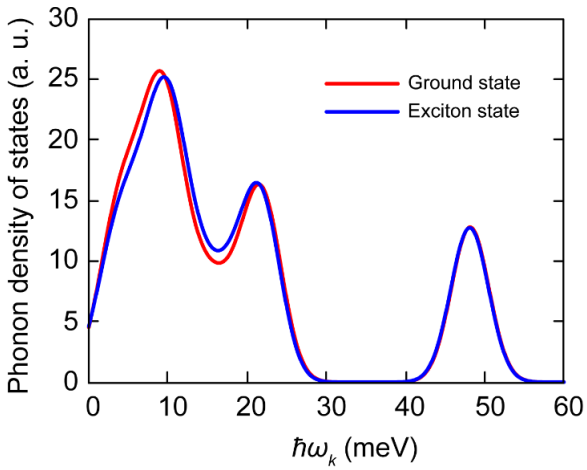

Figure S1. Phonon density of states (PDOS) of ground-state (red line) and excited-state (blue lnie) of 1.5 nm *sp*-ZB NCs.

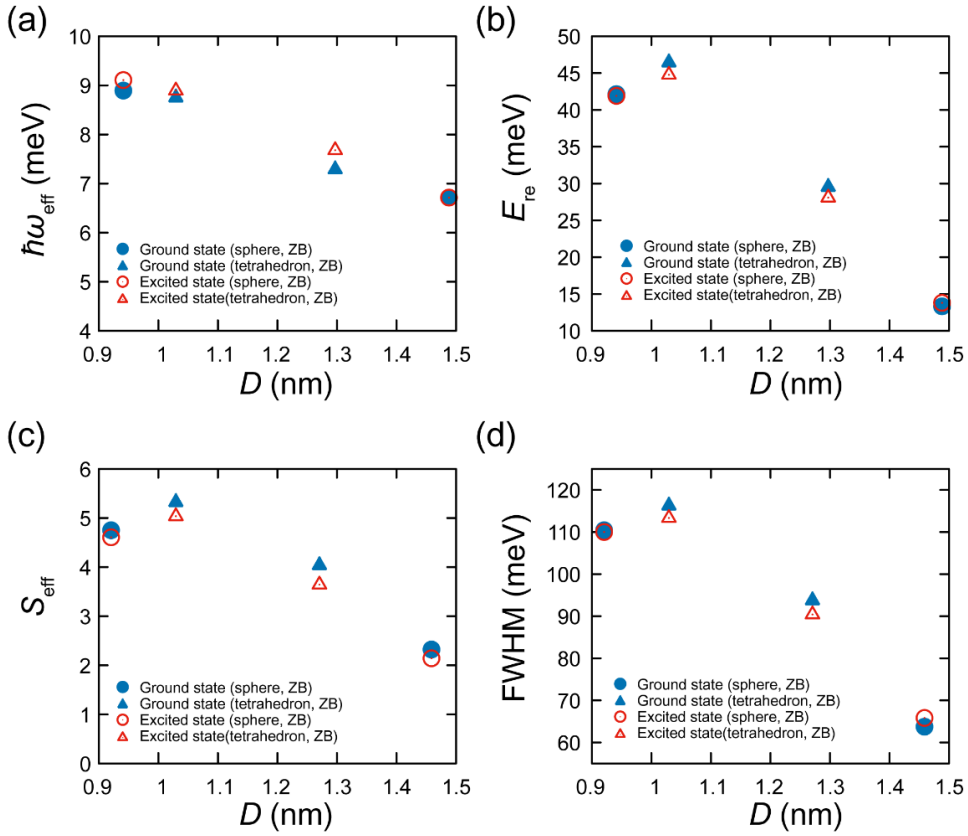

Figure S2. (a) $\hbar\omega_{eff}$, (b) E_{re}, (c) S_{eff} and (d) FWHM calculated by ground state phonon modes (blue dots) and excited state phonon modes (red dots).

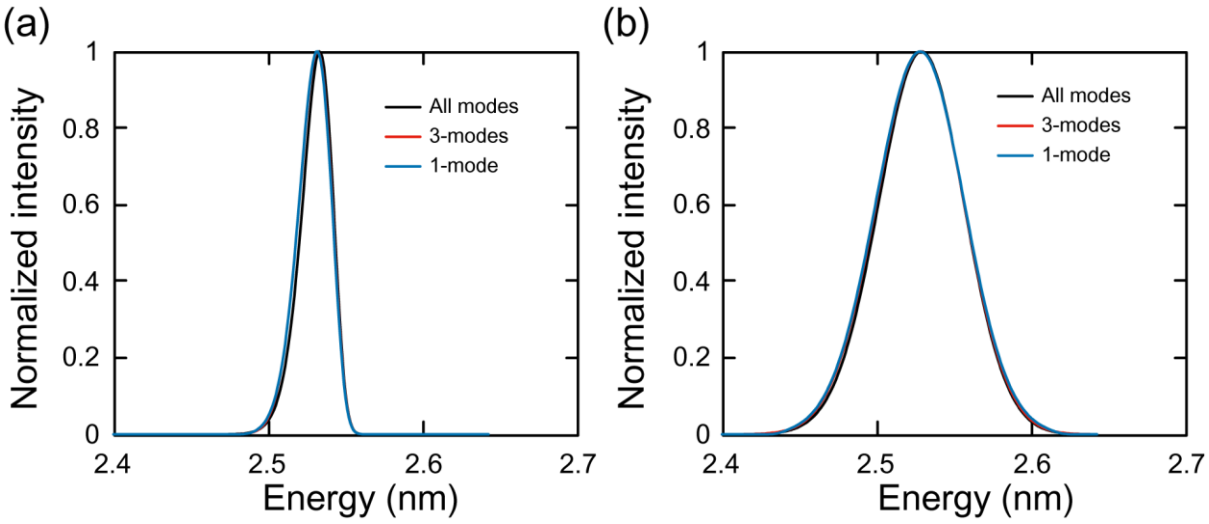

Figure S3. The line spectra of 1.5 nm spherical ZB CdSe NCs calculated in (a) 5 K and (b) 300 K. The line spectra calculated by considering all modes (black lines) are compared to those calculated by effective mode approximations to reduce number of modes to three (red lines) and one (blue lines).

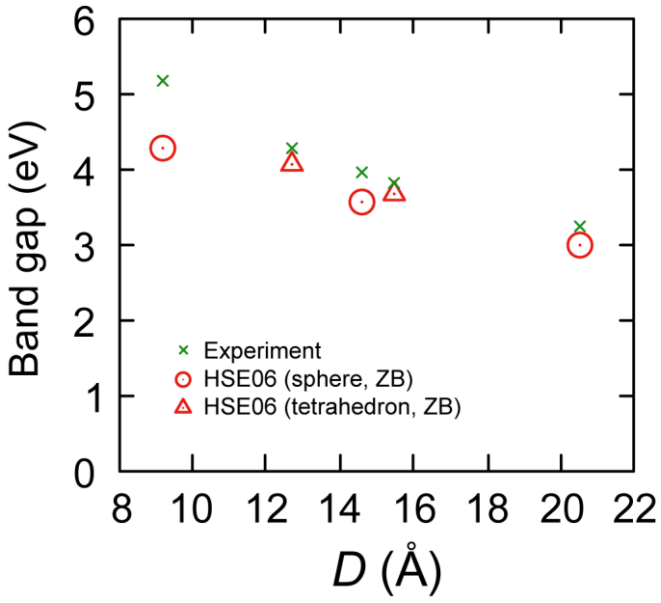

Figure S4. Fundamental band gap estimated from the experimental data (green dots) and calculated by HSE06 functional (red dots). Experimental fundamental band gaps are obtained by summing optical band gap estimated from ref. S7, and exciton binding energy estimated from ref. S8 and S9.

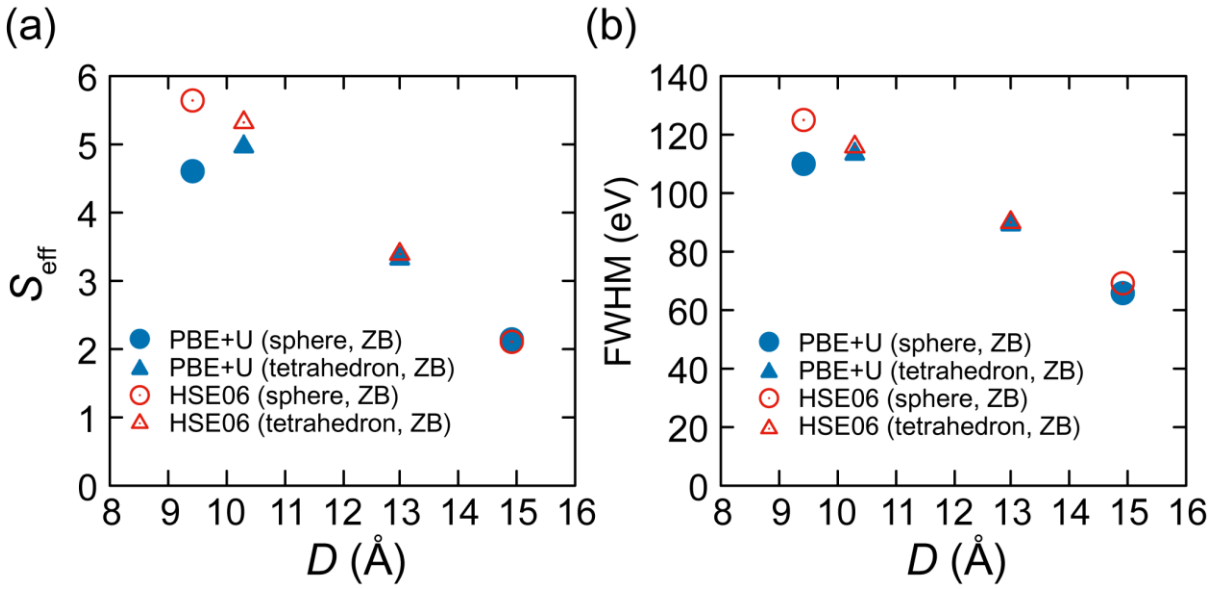

Figure S5. (a) S_{eff} and (b) FWHMs of CdSe NCs calculated by PBE+U (blue dots) and HSE06 functional (red dots). The fraction of the exact exchange energy is set to 0.25 to fit the experimental band gap (discussed in the caption of Figure S4).

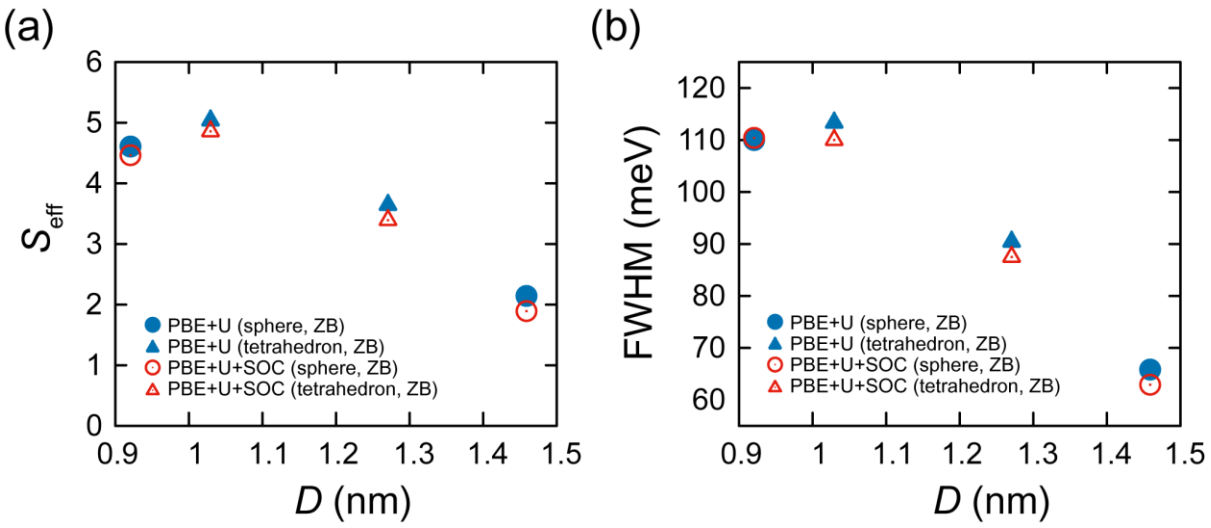

Figure S6. (a) S_{eff} and (b) FWHM calculated with GGA+U functional with (red dots) and without (blue dots) considering SOC.

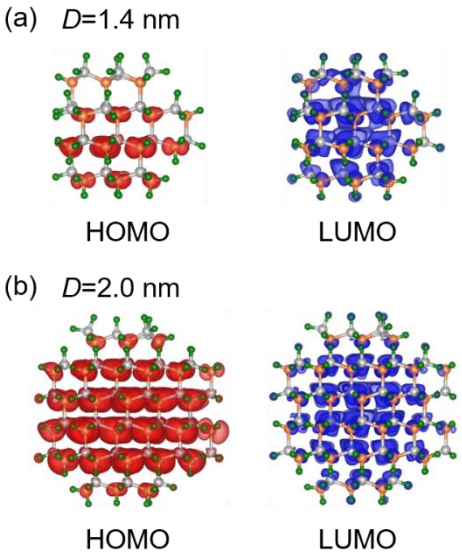

Figure S7. HOMO and LUMO of (a) 1.4 nm and (b) 2.0 nm *sp*-WZ NC.

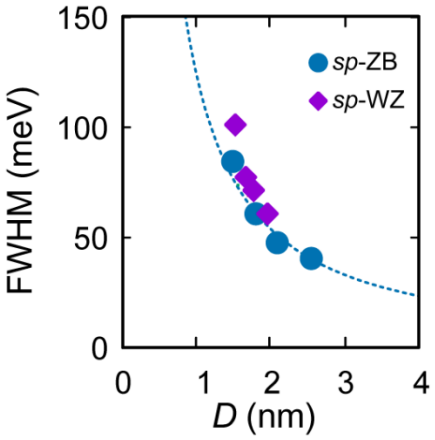

Figure S8. FWHM in *sp*-ZB and *sp*-WZ NCs with respect to *D*.

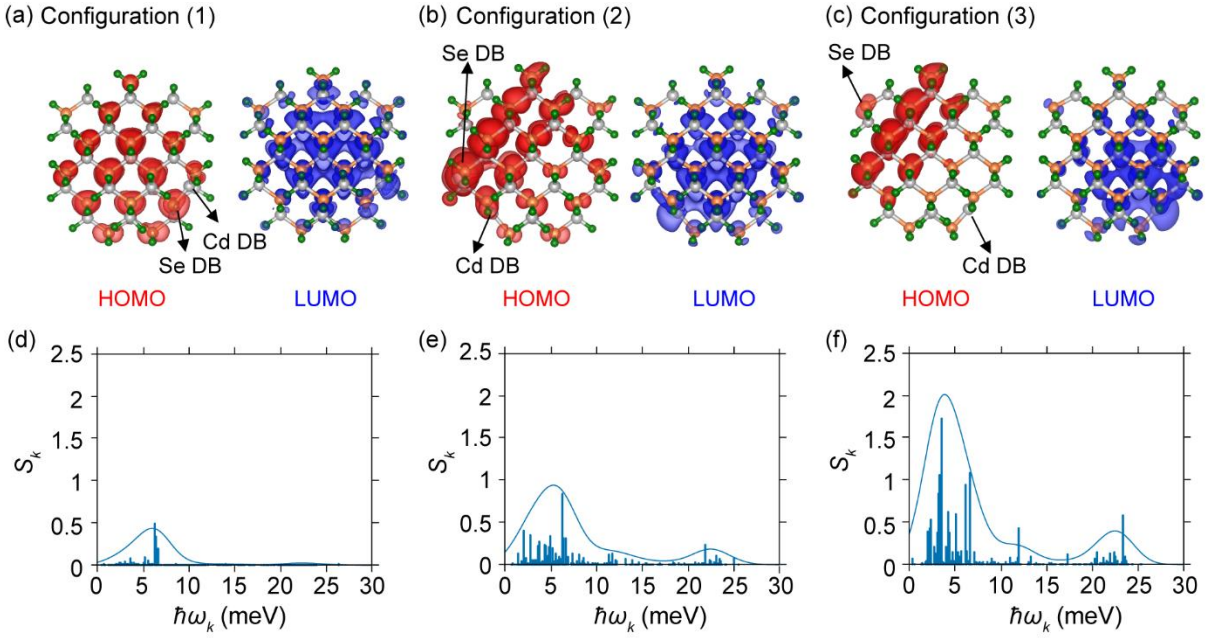

Figure S9. (a-c) Distribution of HOMO and LUMO for 1.5 nm *sp*-ZB NC with different defect configurations. Dangling bonds (DBs) are pointed by arrows. (d-f) Partial Huang-Rhys factors for corresponding configurations in a-c, respectively.

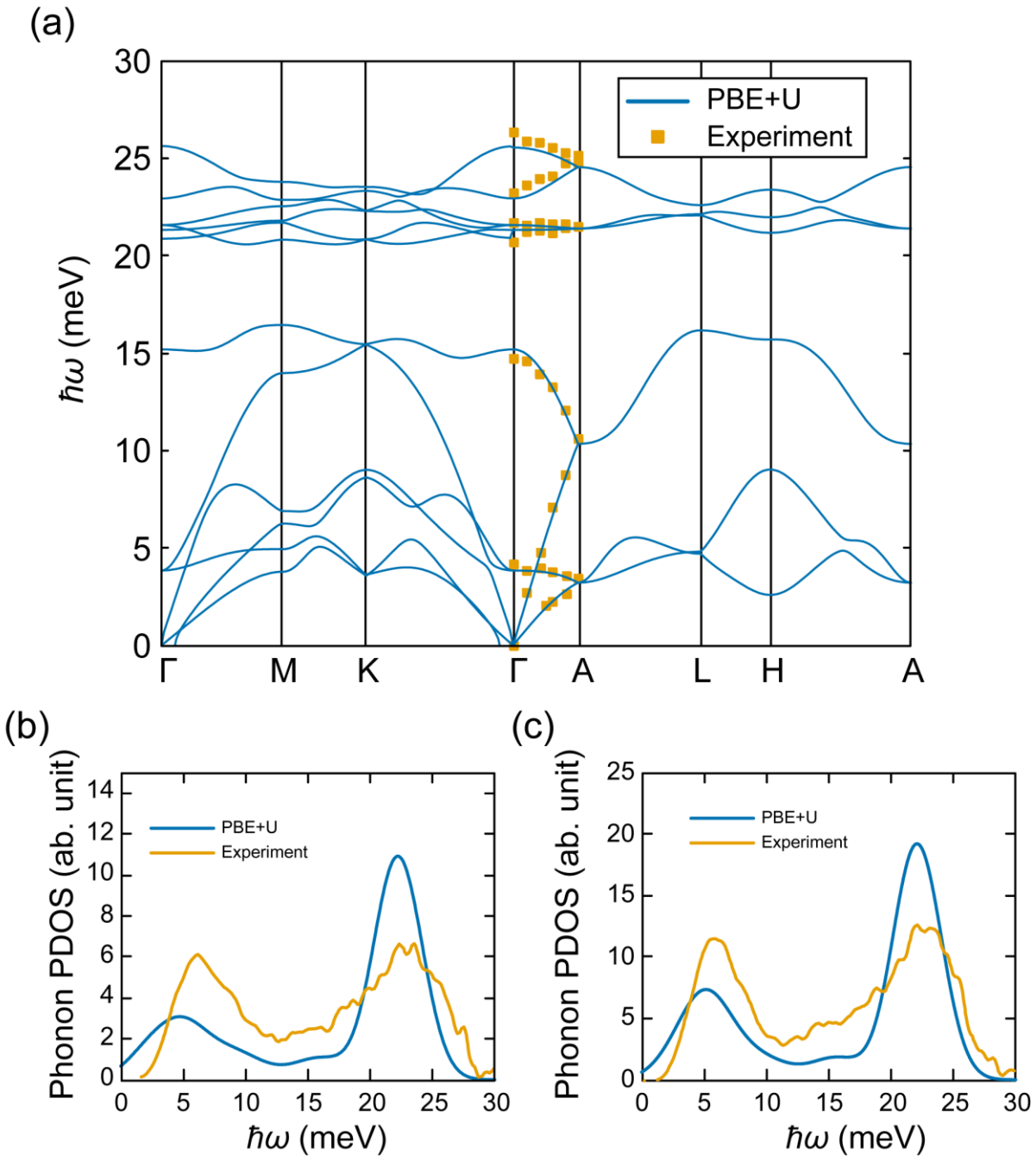

Figure S10. (a) Phonon band calculated by PBE+*U* functional compared with the experiment [S11]. The calculated phonon partial density of states (PDOS) of tetrahedral CdSe ZB NCs of diameter (b) 1.30 nm and (c) 1.57 nm compared to the high energy resolution inelastic x-ray scattering experiments [S5].

Table S1. FWHMs of 1.5 nm NCs with various defect configurations. Configurations (1)-(3) refer to the defect structures presented in Figures S9a-c, respectively.

Defect configuration	FWHM (meV)
Without defect	84
Configuration (1)	95
Configuration (2)	103
Configuration (3)	180

Table S2. Cutoff energy dependence of E_{re} and FWHM in units of meV for a 1.5 nm *sp*-ZB NC.

Cutoff energy (eV)	E_{re} (meV)	FWHM (meV)
300	14.6	65.3
350	15.6	67.5
400	15.6	67.6

Table S3. Lattice parameters of bulk CdSe calculated by GGA+*U* functional compared with the experimental values.

	GGA+*U*	Experiment [S10]
Bulk WZ CdSe	a = 4.28 Å c = 6.97 Å	a = 4.30 Å c = 7.01 Å
Bulk ZB CdSe	a = 6.03 Å	a = 6.05 Å

Table S4. The dependence of calculation results on pseudo-hydrogen mass of 1.49 nm spherical ZB CdSe NCs.

Pseudo-H mass (amu)	$\hbar\omega_{\text{eff}}$ (meV)	S_{eff}	FWHM (meV)
1	6.9	1.96	65
16	5.9	2.12	66
32	5.2	2.96	68
64	4.3	3.55	68

Table S5. The values of σ and E_{ZPL} used to calculate the FWHM in Figure 4b, c and d in the main text. E_{ZPL} is chosen so that the emission peak is similar to the experimental absorption peak estimated from ref. S7.

		D (nm)	E_{ZPL} (eV)	σ (meV)
Tetrahedral ZB	$Cd_{20}Se_{10}H_{40}$	1.03	3.68	7
	$Cd_{35}Se_{20}H_{60}$	1.30	3.33	7
	$Cd_{56}Se_{35}H_{84}$	1.57	3.05	5
Spherical ZB	$Cd_{13}Se_{16}H_{12}H_{24}$	0.94	3.86	7
	$Cd_{43}Se_{44}H_{36}H_{40}$	1.49	3.13	5
	$Cd_{83}Se_{80}H_{64}H_{52}$	1.81	2.83	4
	$Cd_{116}Se_{104}H_{96}H_{48}$	2.09	2.68	4
	$Cd_{201}Se_{176}H_{148}H_{48}$	2.54	2.47	2
Spheroidal ZB	$Cd_{61}Se_{56}H_{56}H_{36}$	1.66	2.95	5
	$Cd_{101}Se_{108}H_{60}H_{88}$	2.10	2.64	3
	$Cd_{145}Se_{132}H_{112}H_{60}$	2.33	2.53	3
Spherical WZ	$Cd_{51}Se_{51}H_{61}H_{21}$	1.53	3.13	7
	$Cd_{57}Se_{62}H_{37}H_{57}$	1.66	2.95	5
	$Cd_{75}Se_{69}H_{66}H_{42}$	1.79	2.84	4
	$Cd_{93}Se_{93}H_{63}H_{63}$	1.96	2.74	4

References

[S1] Kresse, G.; Furthmüller, J. Efficient Iterative Schemes for Ab Initio Total-Energy Calculations Using a Plane-Wave Basis Set. *Phys. Rev. B* **1996**, *54* (16), 11169–11186.

[S2] Kresse, G.; Joubert, D. From Ultrasoft Pseudopotentials to the Projector Augmented-Wave Method. *Phys. Rev. B* **1999**, *59* (3), 1758–1774.

[S3] Perdew, J. P.; Burke, K.; Ernzerhof, M. Generalized Gradient Approximation Made Simple. *Phys. Rev. Lett.* **1996**, *77* (18), 3865–3868.

[S4] Dudarev, S.; Botton, G. Electron-Energy-Loss Spectra and the Structural Stability of Nickel Oxide: An LSDA+U Study. *Phys. Rev. B* **1998**, *57* (3), 1505–1509.

[S5] Shi, C.; Beecher, A. N.; Li, Y.; Owen, J. S.; Leu, B. M.; Said, A. H.; Hu, M. Y.; Billinge, S. J. L. Size-Dependent Lattice Dynamics of Atomically Precise Cadmium Selenide Quantum Dots. *Phys. Rev. Lett.* **2019**, *122* (2), 026101.

[S6] Alkauskas, A.; Buckley, B. B.; Awschalom, D. D.; Van de Walle, C. G.; First-principles theory of the luminescence lineshape for the triplet transition in diamond NV centres. **2014** *New J. Phys. 16* (7), 073026.

[S7] Yu, W. W.; Qu, L.; Guo, W.; Peng, X. Experimental Determination of the Extinction Coefficient of CdTe, CdSe, and CdS Nanocrystals. *Chem. Mater.* **2003**, *15* (14), 2854–2860.

[S8] Meulenberg, R. W.; Lee, J. R. I.; Wolcott, A.; Zhang, J. Z.; Terminello, L. J.; van Buuren, T. Determination of the Exciton Binding Energy in CdSe Quantum Dots. *ACS Nano* **2009**, *3* (2), 325-330.

[S9] Jasieniak, J.; Califano, M.; Watkins, S. E.; Size-Dependent Valence and Conduction Band-Edge Energies of Semiconductor Nanocrystals. *ACS Nano* **2011**, *5* (7), 5888-5902.

[S10] Madelung, O.; Schulz, M.; Weiss, H.; Landolt-Börstein (Eds.) Numberical Data and Functional Relationships in Science and Technology, vol. 17, Springer, Berlin (1982).

[S11] Widulle, F.; Kramp, S.; Pyka, N. M.; Göbel, A.; Ruf, T.; Debernardi, A.; Lauck, R.; Cardona, M.; The Phonon Dispersion of Wurtzite CdSe. *Physica B* **1999**, *263-264*, 448-451.